Comparing Dynamical Systems by Defective Conjugacy: A symbolic dynamics interpretation of commuter functions.

Erik M. Bollt* and Joseph D. Skufca†
Department of Mathematics, Clarkson University, Potsdam, New York, 13699-5815
(Dated: June 18, 2009)

While the field of dynamical systems has been focused on properties which are invariant to "good" change of variables, namely conjugacy, which is an equivalence relationship, when using dynamical systems methods in science and modeling, there lacks a dynamical way to compare dynamical systems, even when they are in some sense "close." In [7, 8], we introduced mathematics to support a philosophy that two dynamical systems should be compared through a change of coordinates between them, that is, a commuter between them which may fail to be a homeomorphism. The progressive degree to which the commuter fails to be a homeomorphism defines what we call a homeomorphic defect. However, at the time of publication of [7, 8], there were limits in the mathematical technology requiring that the transformations be one-dimensional mappings [8] and flows which are well described by such [7], for construction of the commuters by fixed point iteration, and further, difficulties in numerically computing defects in the more complicated one dimensional cases, and further limits to higher dimensional problems. Therefore, here we extend the theory to allow for multivariate transformations, with construction methods separate from the fixed point iteration, and new methods to compute defect. In the course of this work, we introduce several new technical innovations in order to cope with much more general problems. We introduce assignment mappings to understand and illustrate commuters in a broader setting. We discuss the role of symbolic dynamics and coding as related to commuters as well as defect measure. Further, we discuss refinement and convergence of a nested refinement of commuter representations. This work is represents an important practical step forward in the possibility of using the commuter and defects to judge model quality in a wide variety of scientific problems, no longer limited unnaturally by dimensionality and type.

1. INTRODUCTION

To the extent that science seeks to codify knowledge of the world, a fundamental tool in science is the model — a simplified representation of the "true" system under consideration, with mathematical models being a particular example. An essential question within this modeling context is "how close is the model to the true phenomena." Where the natural system under consideration is dynamic, with possibly complex behavior, the field of dynamical systems seeks to provide an appropriate framework for study of these systems. Since the inception of the field of dynamical systems by Henri Poincaré [1], the fundamental approach has been to examine topological and geometric features of orbits, rather than focusing on numerical specifics of particular solutions of the dynamical system, as measured in some specific coordinate system. Characterization of the system relies upon deciphering coordinate independent properties, such as the periodic orbit structure — the count and stability of periodic orbits. Within this dynamical systems framework, the determination of whether two systems are dynamically equivalent is based upon whether or not there is a conjugacy between them [2–6]. However, in any situation where we seek to approximate one thing by another, we need to have some way of quantifying the error in the approximation. Because "conjugacy" is an equivalence relationship, it can not be in the case where one system is only an "approximation" to the original system. The authors have recently introduced a concept of a *communter* which extends to relationships between *non-equivalent* systems [7, 8] and which allows us to define a way to measure the dynamical difference between systems. In this paper, we show the connection between that work and the field of symbol dynamics.

We presume that any model of the "true" system (physical perhaps) is a more simple system (perhaps of ODEs, for example) that is "descriptive" of some aspects of the original. A model should be a system that is somehow easier to analyze. Although the model is only *representative* of the true system, it might

*Electronic address: ebollt@clarkson.edu
†Electronic address: jskufca@clarkson.edu

have been constructed with first principles in mind and may teach us about the mechanisms of the true system. However, the processes of simplication and abstraction (almost invariable) causes the model and the orginal system to be non-equivalent systems, and may be taken as the "norm" in applied mathematics. Consequently, having the means to measure the differences is critical to assessing the accuracy and relevance of a dynamical systems model. Interpretation of dynamical systems through a symbolic representation has become the standard tool for identifying key dynamical structures and behaviors, particularly when studying chaotic systems [2–6]. Consequently, extending and interpreting the concepts of "commuter" and "defect measure" [7, 8] to symbol space is the primary focus of this paper.

This paper is organized as follows:

- In Sec. 2, we provide a short review of the concept of commuters as a way of relating non-equivalent dynamical systems; detailed description of the discussed methods can be found in [7, 8]. The new work of this section is the introduction of a new visualization technique, called an assignment plot. (See Fig. 2.)
- In Sec. 3, we review, in the setting of one-dimensional transformations of the interval, how focusing on how the assumption of a particular topology on the dynamical spaces affects the characteristic details of commuters, conjugacies, and semi-conjugacies.
- In previous work, we showed that uniform contraction of one of the dynamical systems to be compared was a sufficient condition to develop a contraction mapping that would converge to a commuter. In Sec. 4, we extend those results to require only that one of the systems has a generating partition. The proof is demonstrative and leads to the key interpretation of the role of symbol dynamics in comparing non-equivalent dynamical systems.
- Sec. 5, shows the relationship between commuters and coding theory. Additionally, this section provides key results on how to define commuters via a symbol dynamic, how to estimate using periodic orbits, and how to measure the defect between the systems in the symbol space.

2. COMPARING DYNAMICAL SYSTEMS: ON CONJUGACY AND NON-HOMEOMORPHIC COMMUTERS

In the standard approach to dynamical systems theory, the usual way to relate two dynamical systems is with the topological notion of *conjugacy*, represented by the commuting diagram,

$$\begin{array}{ccc} X & \xrightarrow{g_1} & X \\ {\scriptstyle f}\downarrow & & \downarrow{\scriptstyle f} \\ Y & \xrightarrow{g_2} & Y \end{array} . \tag{1}$$

A conjugacy exists if there is a homeomorphism f between the two spaces X and Y which satisfies (1). To be a homeomorphism, f must be one-one, onto, continuous, and its inverse must be continuous. In our recent papers [7, 8], we introduced a relaxed notions of the relationship between the two systems, where we allow that f may fail any one (or several) of the four required properties of homeomorphism while still providing a change of coordinates between the two systems, satisfying

$$f \circ g_1(x) = g_2 \circ f(x). \tag{2}$$

While the preponderance of dynamical systems theory has concentrated on the situation when the two systems g_1 and g_2 are equivalent, as defined in dynamical systems terms by the "commuter"[36], being a homeomorphism, little attention has been paid to the natural scenario that two systems may not be equivalent. One might imagine that if you start with two equivalent systems then continuously perturb some parameter of of those systems, that at the instant they are no longer equivalent, they are still (dynamically) very similar, and ought to be "close" in some sense, a notion not previously defined in a dynamical systems sense before we introduced [7, 8], the measure theoretic concept of *homeomorphic defect,* $\lambda(f)$, which quantifies the difference between the systems by measuring the amount which f may fail to be a homeomorphism.

In our previous work, [8], we showed that when g_2 is uniformly expanding, (and hence g_2^{-1} carries the contraction), then contraction mapping theorem arguments can be used to prove that the fixed point iteration, in terms of the so defined operator, $C_{g_1}^{g_2} f$,

$$f_{n+1}(x) = C_{g_1}^{g_2} f(x) \equiv \hat{g_2}^{-1} \circ f_n \circ g_1(x), \tag{3}$$

converges within a space of bounded functions with respect to the sup-nom, to a function $f_n \to f$, such that f is a commuter, regardless of whether the two maps may be conjugate. In our experience, it apparently converges usefully when g_2 may not be uniformly expanding, but may simply have a positive Lyapunov exponent.

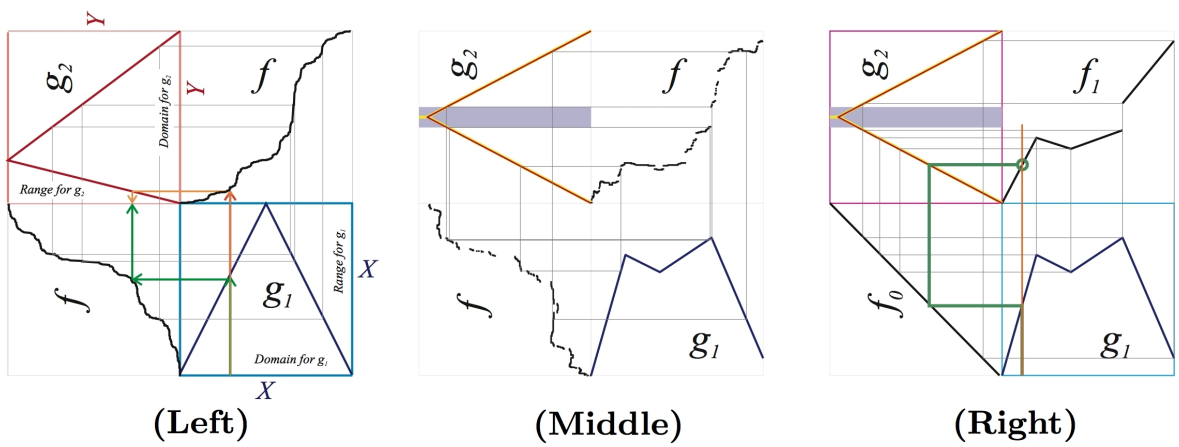

FIG. 1: **(Left) Quadwebs commuting conjugate one dimensional dynamical systems.** The lower right panel shows dynamical system g_1. Since g_1 maps X to X, all four edges of that panel are colored light blue, to indicate that they all describe X, with the domain on the horizontal, and the range on the vertical. System g_2 is plotted in the upper left, but rotated counterclockwise . Again, coloring edges of that panel (pink) represents Y space, with g_2 mapping the vertical domain onto the horizontal range. The commuter f mapping X to Y appears in upper right panel, mapping X to Y. f also appears in the lower left panel, rotated counterclockwise so that it maps range space X to range space Y. Thus, $f \circ g_1(x) = g_2 \circ f(x)$ is shown graphically. Green arrows show a computation of $f \circ g_1(x)$. Orange arrows illutrates graphical computation of $g_2 \circ f$, for the same x. That ends of these arrows must meet indicates that $f \circ g_1 = g_2 \circ f$. Gray rectangles indicate commuting for other x. **(Middle) A non homeomorphic commuter: a vertical gap.** The commuter shown results from partitioning g_1 at its peak. At the x coordinate which is the preimage of that peak, we see a vertical gap in f. Choosing nearby points to the left and right, we will match to g_2 points on either the rising or falling side of the tent, but we cannot match the peak of g_2. The purple rectangle illustrates one of the intervals in g_2 that has no matching dynamics in system g_1. **(Right) Quadweb illustration of the commutation operator in the functional fixed point iteration**. For ease of illustration, we choose f_0 as the identity map, and plot it in the lower left corner. The orange vertical shows a chosen x coordinate, and the green path shows the graphical computation of $g_2^{-1} \circ f \circ g_1(x)$. The intersection in the upper right quad is a point that lies on $f_1(x) = g_2^{-1} \circ f_0 \circ g_1(x)$.

3. REVIEW OF COMMUTER CHARACTERISTICS IN ONE-DIMENSIONAL TRANSFORMATIONS, WITH VARIOUS UNDERLYING TOPOLOGY OF OPEN SETS

In this section, we review some of the characteristics of commuters for non-equivalent systems using one-dimensional dynamics because the resultant defects are easy to visualize and are illustrative of the general setting. To help clarify the intuition behind our methods, we review some typical characteristics of non-homeomorphic commuter functions.

In Fig. 1, we show three commuters between two pairs of dynamical systems. The commuters are conveniently illustrated as it quadwebs, which we introduced in [7, 8] as a way to illustrate the commuting between two one-dimensional dynamical systems whose phase spaces are intervals. While the caption of the figures are somewhat complete descriptions, we further remark,

- **Fig. 1(Left) Quadwebs commuting conjugate one dimensional dynamical systems.** These are two dynamical systems, $g_i : [0,1] \to [0,1]$, which both are full-folding — two-to-one onto the range $[0,1]$. These maps are conjugate, and the commuter shown is a homeomorphism. However, contrary to popular conception (as mislead by the ever popular example of a full tent map and a full logistic map[37]), generically, such conjugacies are not smooth. Rather, the commuter, when it is a conjugacy, is generically a Lebesgue singular function. That is, it's derivative exists almost everywhere, but where it exists, it is zero. Nonetheless, being a homeomorphism, and thus satisfying one-one, it manages to rise from 0 to 1.

- **Fig. 1(Middle) A non homeomorphic commuter: a vertical gap.** Nonconjugacy means that the two dynamical systems have orbits which cannot be matched. Specifically, in the picture shown, all of the orbits of the g_2 map which pass through the gray region cannot be matched by any orbit of the g_1 map. Therefore, the gray region and all pre-images of the gray region, leaves a Cantor subset of the unit interval which can be matched by orbits from the g_1 map. Consequently, the commuter function f has vertical jump discontinuities reflecting a range which is a Cantor set. Furthermore, the two-humps of the mapping g_1 requires a nonomotonicity of the commuter f, as results when matching to a one-humped g_2. The failing of the commuter f to be a homeomorphism, and the manner in which it fails, (no continuity, no one-one, no onto) each reflect a manner of non matching of some portion of the dynamics of one or the other dynamical systems. Measuring the failing, relatively through chosen measures, has lead to our definitions of defect measure [8].

- **Fig. 1(Right) Quadweb illustration of the commutation operator in the functional fixed point iteration**. The fixed point iteration, Eq. (3), can be illustrated graphically, also by a quadweb. Here, the identity function is shown as the initial function f_0. The only requirement of a suitable initial f_0 being that it satisfy the boundary conditions shown. As shown, the fixed point iteration occurs point-wise. The two major homeomorphic defects features of the commuter, the discontinuity and lack of onto-ness is due to g_1 not being as tall as g_2, and the non monotonicity implies no one-to-ness, is due to g_1 having two humps while g_2 has only one. Interestingly, in just one iteration, we see generation of the fundamental mismatch, which is propagated on scales in development of the eventual fractal featured commuter.

We now wish to introduce an alternate to Fig. (1) for representing the commuter functions, $f : X \to Y$. Traditionally, functions are shown as a graph of the range over the domain, particularly when X and Y are both subsets of the real line. However, such presentations are not always feasible or useful when the domain and range are not so simple, as we will discuss when X and Y are both attractors, perhaps in R^n. In such case, we define an *assignment plot* which we find to be more useful.

Just as functions are often represented in abstract topological spaces by arrows running from points in the domain to points in the range, an assignment plot shows line segments from representative points in X, under f to their images in Y. This graphical presentation works equally well for the one dimensional commuters described in this section as they will for the multivariate transformations in the subsequent sections. As a matter of comparison, we include in Fig. 2, the assignment plots of the commuter already shown in Fig. (1). In Fig. (1), the domain X being a subset of $[0,1]$ is shown at the bottom, and the range Y also being a subset of $[0,1]$ are shown at the top and bottom of the figures. The line segments between show the assignments made by f to a uniform grid of sample points. The tongues like appearance is not surprising, considering the devil's staircase nature of the f already seen. A discontinuity appears as an abrupt loss of "combing", akin to a "cowlick" in a hair style.

4. ON RELAXING UNIFORM EXPANSION FOR ONE-DIMENSIONAL TRANSFORMATIONS

In this section, our goal is to strengthen the results of [7, 8] for the case of 1-d maps of the interval. In particular, we show that if g_2 is piecewise continuous and strictly monotone on each segment, then if the partitioning of Y by these monotone laps is *generating* then our iterative method converges to a solution to the commutative diagram which is uniquely determine by the choice of what part of X space is match to each of the partition elements of Y. These conditions are essentially equivalent to the requiring that the g_2 dynamics be sensitively dependent on initial condition. Our proof uses symbol dynamics, leading to

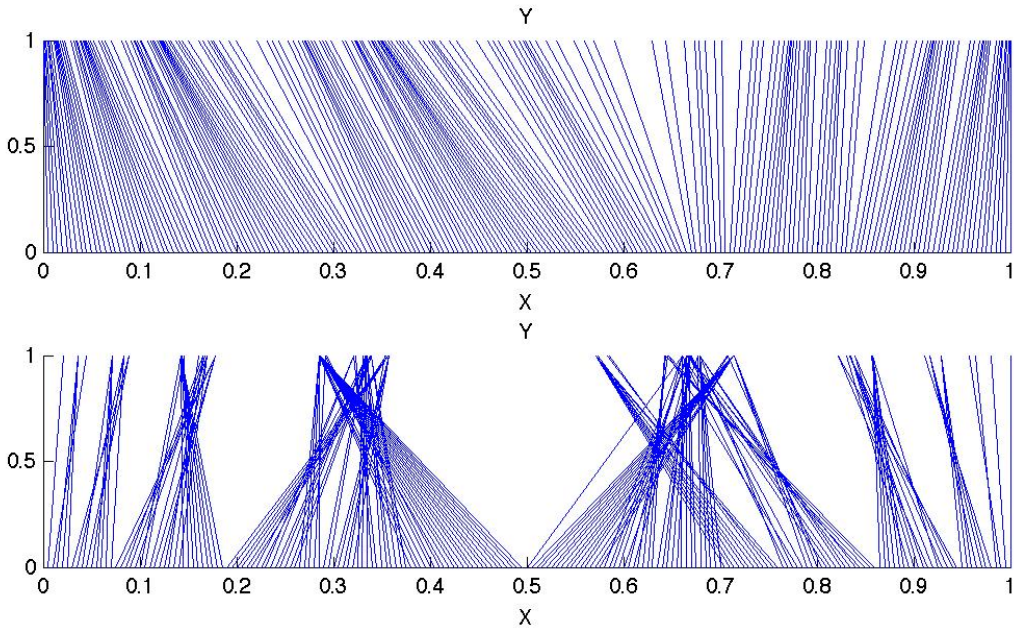

FIG. 2: **An Assignment Plot** of one dimensional mappings $f : X \to Y$, with the domain $X \subset [0,1]$ shown at the bottom, and the range $Y = [0,1]$ shown at the top. Line segments show an assignment from X to Y of a uniform grid of sample points representing the commuters f. The **Top** assignment plot represents the conjugacy function between two tent maps already seen in Fig. 1, where the graph shown in the quadweb illustrated a Lebesgue singular function. The **Bottom** assignment plot represents the non homeomorphic commuter function shown in the quadweb in Fig. 1, between a tent map, and a two-humped map. Especially apparent with this function which is not a homeomorphism is the nonmonotonicity, apparent as crossing lines.

a natural demonstration that the commuter matches points in X to points in Y such that the respective symbol dynamics will match for as many iterates as possible.

A. Setting, background, and notation

We specialize to 1-d maps of the interval. To further ease notation, we assume (without further loss of generality) that $g_1 : [0,1] \to [0,1]$ and $g_2 : [0,1] \to [0,1]$. Additionally, we require that g_2 be piecewise continuous and also piecewise strictly monotone (no horizontal segments in the graph of g_2. We seek to describe function f that satisfies the commutative diagram

$$\begin{array}{ccc} X & \xrightarrow{g_1} & X \\ {\scriptstyle f}\downarrow & & \downarrow{\scriptstyle f} \\ Y & \xrightarrow{g_2} & Y, \end{array} \tag{4}$$

equivalent to the requirement

$$f \circ g_1 = g_2 \circ f. \tag{5}$$

In particular, we focus on the iterative solution described in [8], which we outline below.

Let n be the number of monotone laps of g_2. Let $\mathcal{P}_y$ be the closed interval partion of $[0,1]$ into n strictly monotone subintervals. Denote the end points of these intervals as $0 = y_0 < y_1 < \ldots < y_n = 1$, with $E_y = \{y_0, \ldots, y_n\}$. Define restriction

$$g_{2i} = g_2|_{[y_{i-1}, y_i]}.$$

Because this restriction is strictly monontone, it is invertible. We define the extension of this inversion, denoted $\hat{g}_{2i}^{-1}$, as the continuous, monotone extension of g_{2i}^{-1} to the domain $[0,1]$ satisfying

$$\frac{\mathrm{d}\hat{g}_{2i}^{-1}(y)}{\mathrm{d}y} = 0 \qquad \text{for } y \text{ not in the range of } g_{2i}.$$

(The above requirement is equivalent to specifiy vertical "zeds" [8].)

Let $\{I_{Y_i}\}_{1=1}^n$ be a disjoint set of subintervals of $Y = [0,1]$ that cover this interval, where the subscript i denotes that y_{i-1} and y_i are the endpoints of that subinterval. Let $\{I_{X_i}\}_{1=1}^n$ be a disjoint set of subintervals of $X = [0,1]$ that cover this interval, where the subscript i is chosen such that our commuter will match points in I_{X_i} with points in I_{Y_i}. Let $\mathcal{F}$ be the set of functions from X to Y, and define the *commutation operator* $C : \mathcal{F} \to \mathcal{F}$ by

$$C\tilde{f}(x) = \hat{g}_{2i}^{-1} \circ \tilde{f} \circ g_1(x), \qquad x \in I_{X_i}. \tag{6}$$

A fixed point f of the commutation operator, satisfying $f = Cf$ will also satisfy the commutative diagram. We attempt to find this fixed point via iteration. Let $f_0 \in \mathcal{F}$ be arbitrary, and let

$$f_{k+1} = Cf_k.$$

We seek to understand *under what conditions does the sequence f_k converge to a fixed point of C.*

For some additional analysis machinery, we borrow from the approach of symbol dynamics and define a sequence of partition refinements of Y by $\mathcal{P}_y^1 = \mathcal{P}_y$, and

$$\mathcal{P}_y^{k+1} = \mathcal{P}_y^k \vee g_2^{-1}\left[\mathcal{P}_y^k\right], \tag{7}$$

where $\vee$ denotes the common refinement. Denote the set of endpoints of these partitions as $E_y^k = \left\{y_0^k, y_1^k, \ldots, y_{n_k}^k\right\}$. The recursive relationship

$$E_y^{k+1} = E_y^k \cup g_2^{-1}[E_y^k] \tag{8}$$

is equivalent to (7). Because the $\hat{g}_{2i}^{-1}$ have vertical extensions (zeds) at the initial partition boundaries, we observe that

$$E_y^1 = \cup_{i=1}^n \hat{g}_{2i}^{-1}([0,1]) \subset \bigcup_{i=1}^n \hat{g}_{2i}^{-1}[E_y^1],$$

so that

$$E_y^2 = E_y^1 \cup g_2^{-1}[E_y^1] = \bigcup_{i=1}^n \hat{g}_{2i}^{-1}[E_y^1].$$

Continuing this argument by induction gives the alternative representation

$$\mathcal{P}_y^{k+1} = \bigcup_{i=1}^n \hat{g}_{2i}^{-1}\left[\mathcal{P}_y^k\right], \tag{9}$$

B. Bounding the commuter

Our goal in this section is to establish upper and lower bounds for a fixed point of the commutation operator, which we will define via a sequence of bounding functions. We use those bounds to show that if the partition norm $|\mathcal{P}_y^k| \to 0$, the commutation operator converges to a fixed point.

Let $M_0(x) = 1$ and $m_0(x) = 0$. Then for arbitrary $f_0 \in \mathcal{F}$, we have $m_0(x) \leq f_0(x) \leq M_0(x)$. Define recursively the sequence of functions

$$M_{k+1}(x) = \max\left\{\hat{g}_{2i}^{-1}\left([m_k(g_1(x)), M_k(g_1(x))]\right)\right\}, \tag{10}$$

$$m_{k+1}(x) = \min\left\{\hat{g}_{2i}^{-1}\left([m_k(g_1(x)), M_k(g_1(x))]\right)\right\}, \qquad x \in I_{X_i}. \tag{11}$$

As a result of the monotonicity of $\hat{g}_{2i}^{-1}$, we make the following observations:

- An equivalent formulation is given by

$$M_{k+1}(x) = \max(Cm_k(x), CM_k(x)) \tag{12}$$
$$m_{k+1}(x) = \min(Cm_k(x), CM_k(x)), \tag{13}$$

  where in these equations, we mean for the max (or min) to be taken over the two possible values (not the open interval), because maximum and minimum values must occur at endpoints.

- As values, we observe that $\forall x, M_1(x) \in E_1$, the set of edge points of the initial partition, and similarly for $m_1(x)$. Since further iterations are produced by preimage under $\hat{g}_{2i}^{-1}$, which yields the same values as computed under g_2^{-1}, by induction, we have $M_k(x) \in E_k$ and $m_k(x) \in E_k$.

- If $m_k(x) = M_k(x)$, then the closed interval in (10),(11) degenerates to a singleton. It immediately follows that $m_K(x) = M_K(x) \quad \forall K \geq k$.

- If $m_k(x) < M_k(x)$, then the interval $[m_k(x), M_k(x)]$ is a partition element of $\mathcal{P}_y^k$. In other words, there is no $y \in E_y^k$ such that $m_k(x) < y < M_k(x)$, established by simple induction using (9).

- We observe that at each for each x, we start by maximizing (or minimizing) $\hat{g}_{2i}^{-1}$ over its domain, $[0, 1]$. Under iteration, the resultant interval $[m_1(x), M_1(x)]$ must be a subset of $[0, 1]$ for every value of x. Under continued iteration (applying (10) and (11)), we are always finding extreme values of the same function, but over an interval that is a subset of the original. The resultant intervals, therefore, must be nested. By induction, one easily sees that $m_k(x) \leq f_k(x) \leq M_k(x)$, yielding the nesting statement,

$$m_0(x) \leq m_1(x) \leq \ldots \leq m_k(x) \leq f_k(x) \leq M_k(x) \leq M_{k-1}(x) \leq \ldots \leq M_0(x), \qquad \forall k = 1, 2, \ldots, \quad \forall x. \tag{14}$$

  By monotone convergence, we have $M_k(x) \to f^+(x)$, and $m_k(x) \to f^-(x)$, where f^+ and f^- must bound the $\lim f_k$, if that limit exists.

Lemma 1. *If partition norm $|\mathcal{P}_y^k| \to 0$ then the sequence $f_k(x) \to f(x)$ uniformly.*

Proof. From (14), we have that

$$m_k(x) \leq f_k(x) \leq M_k(x).$$

Since either $m_k(x) = M_k(x)$ or those points fall on a partition boundary of $\mathcal{P}_y^k$, we have

$$M_k(x) - m_k(x) \leq |\mathcal{P}_y^k| \to 0,$$

with this bound independent of x. Therefore $M_k(x) \to f^+(x)$ and $m_k(x) \to f^-(x)$ implies $f^+(x) = f^-(x)$. By squeeze theorem, $f(x) = f^+(x) = f^-(x)$, with uniform convergence, yielding the fixed point of the commutation operator. □

The discussion here has regarded nesting of intervals, which we have carefully stated our assumptions as such but without further assuming contraction, it cannot be shown to follow that a given nested sequence of intervals converges to a singleton. This is no different from the usual situation in symbolic dynamics, when discussing conjugacy or semiconjugacy to symbolic shift spaces, by a generating partition, or simply a Markov partition.

C. Symbol dynamics interpretation of the commuter

To define symbol dynamics for our systems, we assume a shift space on Σ_n, with integer symbols $1, \ldots, n$. We assocaiate symbol i with interval I_{X_i} for the dynamics on X and with $[y_{i-1}, y_i]$ for the dynamics on Y. A trajectory of system g_1, given by $\{x, g_1(x), g_1^2(x), \ldots\}$ has an associated symbolic trajectory $\sigma^x = \sigma_0^x.\sigma_1^x, \ldots,$ where $g_1^j(x) \in I_{X_i} \implies \sigma_j^x = i$. Similarly, a trajectory of system g_2, given by $\{y, g_2(y), g_2^2(y), \ldots\}$ has an associated symbolic trajectory $\sigma^y = \sigma_0^y.\sigma_1^y, \ldots,$ where $g_2^j(y) \in [y_{i-1}, y_i] \implies \sigma_j^x = i$. We remark that because the closed partition on Y gives an overlap at endpoints, the symbolic trajectory is non-unique for

any preimage of any element of E_y. We denote Σ^y as the set of all possible symbolic sequences for y. We take the distance between two symbolic sequences to be the standard metric on Σ_p, given by

$$d(\sigma, \tilde{\sigma}) = \sum_{k=0}^{\infty} \frac{\delta(\sigma_k, \tilde{\sigma}_k)}{p^k},$$

where δ is the Kroneker delta. Because of the non-unique symbol sequences on Y, we define

$$d(\sigma^x, \Sigma^y) = \inf_{\sigma^y \in \Sigma_y} d(\sigma^x, \sigma^y).$$

Lemma 2. *If $m_k(x) < M_k(x)$, then the interval $[m_k(x), M_k(x)] \subset Y$ is the subinterval of Y associated to the first k symbols of σ^x.*

Proof. The process for construction of $\mathcal{P}_y^k$ is exactly the symbol dynamics method for constructing the intervals associated to length k symbolic words , and these partition intervals match to $[m_k(\cdot), M_k(\cdot)]$, as discussed above. So we need to show that the process matches x to the *correct* sequence of partition intervals.

By induction: Choose arbitrary (but fixed) x, with symbolic representation $\sigma^x = \sigma_0^x.\sigma_1^x, \ldots$.

- **True for** $k = 1$: Interval $[m_1(x), M_1(x)] = \hat{g}_{2\sigma_0}^{-1}([0, 1]) = [y_{\sigma_0 - 1}, y_{\sigma_0}]$, where we have already designated that this subinterval in Y is associated to symbol σ_0.
- **Induction assumption (A)**: Assume that for every x s.t. $m_k(x) < M_k(x)$, the interval $[m_k(x), M_k(x)]$ designates that interval of Y associated to the first k symbols of σ^x.
- **Implies true for** $k + 1$**:** We need to show that $m_{k+1}(x) < M_{k+1}(x)$ implies that the symbol associated to this interval in Y space is the $k+1$ symbol of the symbol itinerary of x. We proceed as follows:

  From (10) and (11), we know strict inequality $m_{k+1}(x) < M_{k+1}(x)$ holds only only if

  $$m_k(g_1(x)) < M_k(g_1(x)). \tag{15}$$

  Denoting $x_1 = g_1(x)$, inequality (15) allows us to apply induction assumption (A) at the point x_1, which implies a length k symbol match at for the interval $[m_k(x_1), M_k(x_1)]$, associating to the word $\sigma_1^x, \ldots, \sigma_k^x$, the first k simbols of the first shift on σ_x. The operations of (10) and (11) of applying $\hat{g}_{2i}^{-1}$ guarantee that the first symbol is correct, so that $[m_{k+1}(x), M_{k+1}(x)] \subset Y$ associates to the length $k + 1$ word $\sigma_0^x, \ldots, \sigma_k^x$.

□

Lemma 3. *Suppose $\mathcal{P}_y^k \to 0$ so that $f_k \to f$, yielding the commuter function $f(x)$. If $y_0 = f(x_0)$ then*

$$d(\sigma^{x_0}, \Sigma^{y_0}) \leq d(\sigma^{x_0}, \Sigma^y) \qquad \forall y \in Y.$$

In other words, the symbolic representation of y_0 matches the representation for x_0 for as many (leading) symbols as is possible before the first non-matching symbol.

Proof. By induction: Suppose σ^{y_0} matches σ^{x_0} for the first k symbols. We want to show that either

1. The symbol sequences match for the first $k + 1$ symbols, or
2. No point $y \in I_y$ will match for $k + 1$ symbols.

Case 1: If the sequences also match for $k + 1$ symbols, then continue by induction, incrementing k. If $k \to \infty$, then proof complete.

Case 2: Assume that σ^y does not match σ^x at the $k + 1$ symbol. Applying Lemma 2, we lack of match at symbol $k + 1$ implies that a strict inequality for the upper and lower bounds is not possible, so that $m_{k+1}(x_0) = M_{k+1}(x_0)$. So there is no proper subinterval of Y that matches for $k + 1$ symbols, and no point in Y can match for $k + 1$ symbols, except possibly $y = m_{k+1}(x_0) = M_{k+1}(x_0) = f(x_0)$, as demonstrated in Lemma 1. □

D. Implications of Lemmas 1-3.

The direct intent of this section was to extend the class of problems for which we could show that the iterative scheme indicated by (3) will converged to a fixed point. Our revised requirement for a certain class of 1-d maps is that the dynamics of g_2 admit a generating partition. The process detailed in [8] yields a *unique* commuter only after one has assigned an appropriate relationship between the partitioning of the spaces X and Y. The results of this section, prove that for the 1-d maps considered, the resultant commuter provides an optimal matching of the associated symbol dynamics. In the following sections, we argue that this property of commuters should be preserved in the general, higher dimensional setting. Figure 3 illustrates this characterization of the commuter as providing a match between the symbol dynamics of the systems.

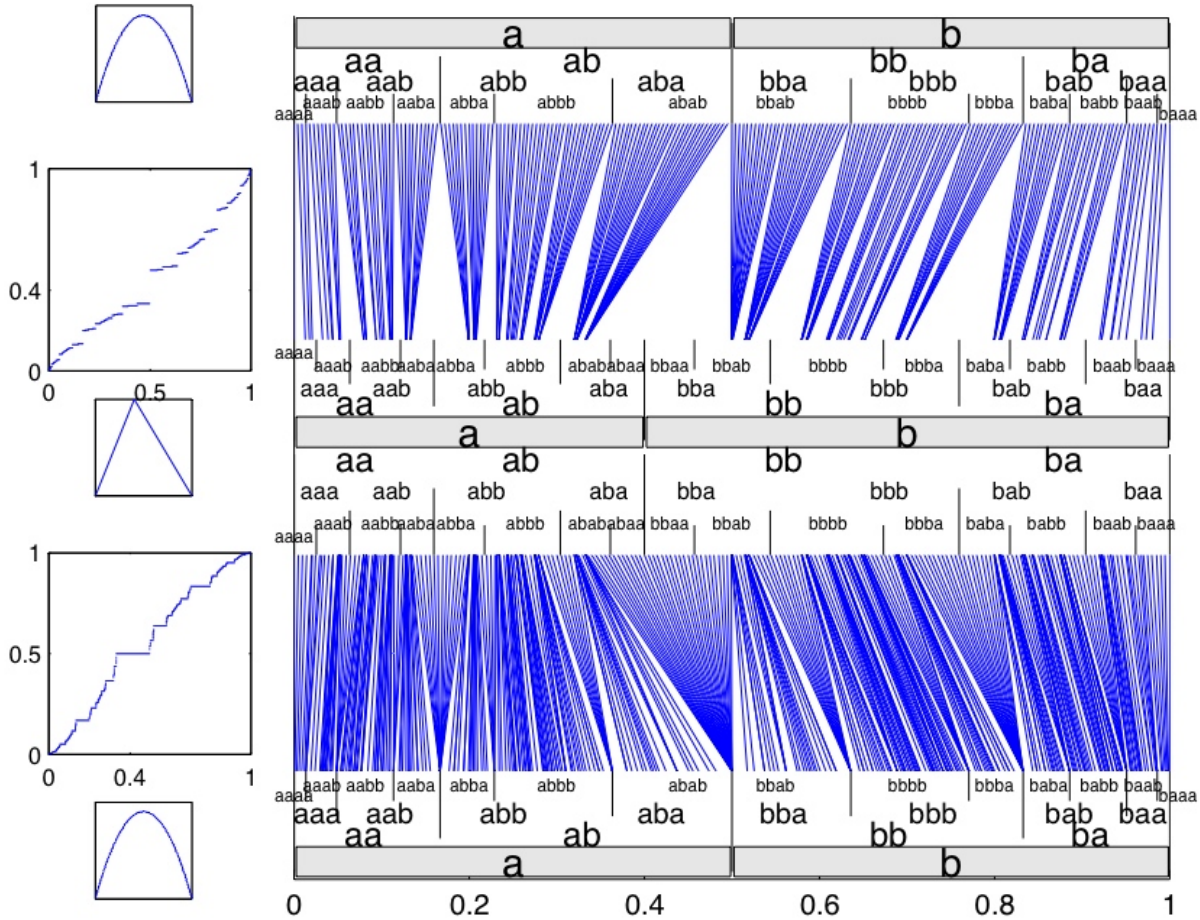

FIG. 3: **Commuter as the matching of symbol dynamics.** (Left) Down the left side of this diagram is a sequence of maps: (1) $g_1 = 3.6x(1-x)$,a subshift logistic map; (2) the commuter between g_1 and (3) the full shift skew-tent map g_2; (4) the commuter from g_2 back to (5) map g_1. (Right) On the right side, we show the symbol dynamic partition of the unit interval for maps g_1 (at top and bottom) and g_2 (in the middle), where we show all intervals for word length of four or fewer symbols. The assignment plot (blue lines) is taken from the commuters between the maps (as computed from the fixed point iteration), and shows that the commuter also gives a symbolic dynamic match between the two systems. *Observe:* (1) Map g_1 admits neither *abaa* nor *bbaa*, associated to the largest vertical gap in the first commuter. (2) Because g_2 is a full shift on two symbols, the words *abaa* and *bbaa* exist in the dynamics of g_2, but cannot be "matched" to a depth of four symbols with any point of g_1. Those intervals associate to the largest horizontal portion of the second commuter. The commuter maps those points to 0.5, on the boundary between symbols a and b of the g_1 dynamics, yielding a match to a depth of three symbols, either *aba* of *bba* as appropriate. This mapping of intervals to a single point associates to $m_k(x) = M_k(x)$, instead of a strict inequality between the bounding functions.

5. ON SYMBOLIC DYNAMICS MATCHING, CODING THEORY, FINITE EQUIVALENCE, AND DEFINITION OF COMMUTERS VIA SYMBOL DYNAMICS

Consider two Bernoulli shift maps,

$$s_1 : \Sigma'_p \to \Sigma'_p, \text{ and, } s_2 : \Sigma'_q \to \Sigma'_q, \tag{16}$$

where $\Sigma'_p \subset \Sigma_p$ is a subshift[38] and likewise, $\Sigma'_q \subset \Sigma_q$. Then, a commuter between these two dynamical systems on shift spaces, is similarly written, $s_2 \circ f(\sigma) = f \circ s_1(\sigma)$, specializing Eq. (2). While in coding theory, a conjugacy is defined as a commuting change of variables (called a "code" [9]) f, that is invertible, we persist with the stronger definition used in the dynamical systems community called a "topological conjugacy", which is as before, a commuting f that is a homeomorphism. Note that bi-continuity essentially comes for free in the symbol space setting, but surjection (thus called a factor code) and injection (an embedding code) are not automatic.

A useful notion from symbolic dynamics and coding theory is that of "finite equivalence" whereby two shifts, X and Y share a "common extension" W such that there is a finite-one factor code [9] from each, $\phi_X : W \to X$ and $\phi_Y : W \to Y$. In this language, each full skew tent map is finitely equivalent to any other through a common extension 2x mod 1 map by a two-to-one factor code such as shown in Fig. 4(Lower Right). Continuing with this example, we recall [9] the finite equivalence theorem which states that two irreducible sofic shifts are finitely equivalent iff they have the same entropy. As corollary to this statement, there is a theorem [3] that states that adjacency matrices which generate shifts that are finitely equivalent must be similar by nonegative integer matrix similarity transformations.

Although our focus is on non-equivalent dynamics, if we consider the symbol dynamics interpretation of the commuter, these theorems suggest that: (1) when commuting between two dynamical systems of different topological entropy, the transformation must be not always finite-to-one, and (2) in some sense, "permutations" of commuters remain equivalent. By *permutations of the commuter* we simply mean to observe the following: The solution to (2) is not unique; for a unique solution, we must (at a minimum) specify which subsets of X must match to which subsets of Y. If the dynamics do not admit a generating symbol partition (or we choose not to use that partition) there are infinitely many ways to define that matching. Even in the case of known generating partitions, we still have a finite combinatorial choice of matchings. Each such choice leads to a different "permutation" of the commuter. From an application/experimental viewpoint, if we are trying to build data by matching on long trajectories of each of our systems, we may treat each point as if it required its own symbol, so that any matching of an arbitrary point on each trajectory generates a solution to the commutative diagram. In some sense, this extreme symbolization is similar to viewing our original maps from the viewpoint of the discrete topology, where continuity is trivial. From a modeling point of view, we are typically interested in finding a commuter that best "respects" the underlying topologies of the two systems, by which we mean that (optimally) it would be continuous *with respect to these topologies.* In application, that underlying topology would likely be the standard topology or a topology induced by the standard topology.

As an example, to demonstrate and understand the non-uniqueness of commuters, consider the simple example of full shift symmetric tent map, T, and a 2x mod1 map, S, which are semi-conjugate by $T \circ T = T \circ S$. If instead we compare S with a full shift skew tent, the systems are semi-conjugate with respect to the underlying standard topologies [10] of each topological space, with the semi-conjugacy shown in Fig. 4(Lower Right). These systems are also *conjugate* by the commuter functions shown in Fig. 4(Lower Left) and Fig. 4(Upper Right), where *conjugacy* is a result of these functions being continuous with respect to specific orientation reversing topologies. We note that infinitely many such permutations are continuous with to appropriately chosen topologies. However, we contend that a typical modeling problem related to the physical world is likely most relevant with respect to the standard topology.

A. Defining Commuters through Symbol Dynamics

The solution of (2) through fixed point iteration has yielded implementable algorithms to find commuters in the 1-d setting. However, for higher dimensional problems, finding an appropriate contraction is difficult. As an alternative, we may use the insight garnered from Sec. 4 and find commuters through symbol dynamics. We acknowledge identifying generating partitions for the symbol dynamics may be difficult. However, we proceed under the assumption that the dynamical systems under consideration are presented to us with

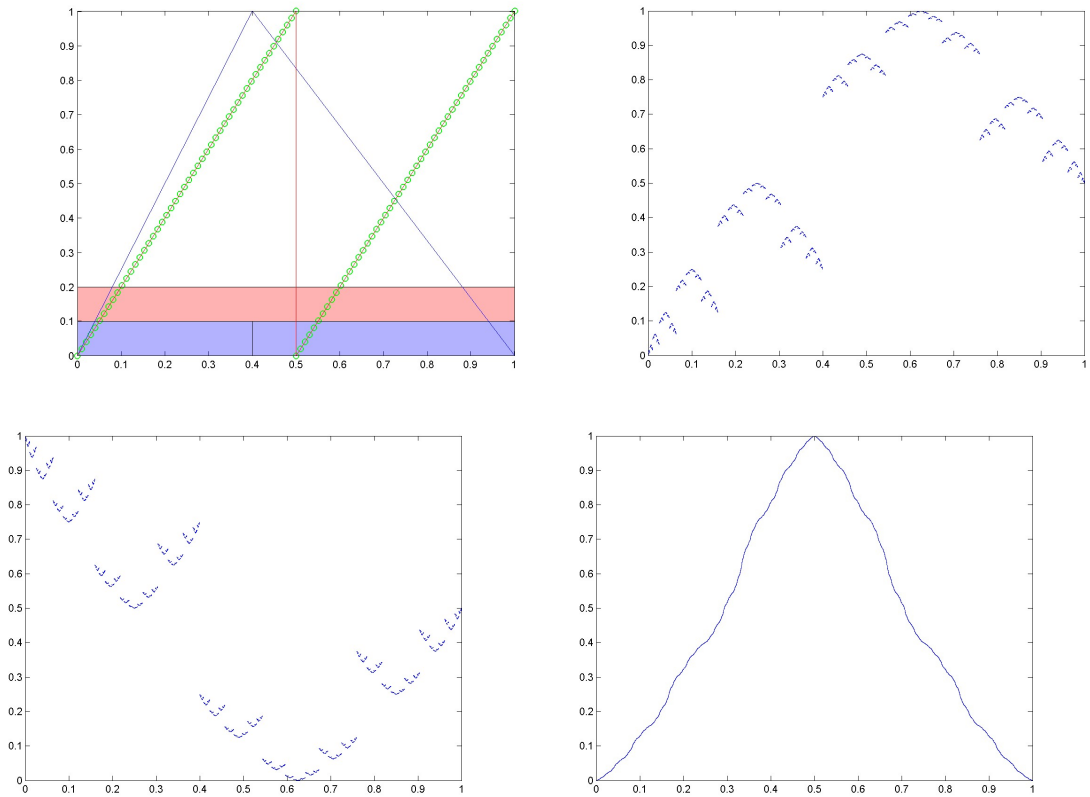

FIG. 4: The skew tent map, T is known to be semiconjugate to the 2x mod 1 map, S, but the semiconjugacy function depends on the choice of topology. (Upper Left) A full skew tent map (blue) and a semiconjugate 2x mod 1 map (green), and the partition elements which are compared, bottom in purple to top in red, as strips along the bottom. (Upper Right) Matching left lap T with left lap of S, and similarly with the right laps of each map generates the illustrated commuter. Although "torn" with respect to standard topology, this commuter is continuous with respect to a reversing order topology, corresponding to Gray code orders. (Lower Left) Matching left laps to right laps between the maps gives another commuter function, which is also continuous, but only with respect to the appropriate topology. (lower Right) In fact, the symmetric tent map is semiconjugate to the 2x mod 1 map by the tent map, $T \circ T = T \circ S$, and similarly, the skew tent map T shown here is semiconjugate to S, by the commuter function shown; this commuter is continuous relative to the standard topology, which can be argued to be the most relevant topology to many modelers. This commuter results from matching $[0, .25) \cup (.751]$ of map S to the left lap of the T, which allows matching of the orientation preserving fixed points. Interval $[.25.75]$ of S is matched to the right lap of T.

a known symbolic dynamic partitioning, with each system represented by dynamics on p symbols, with p finite. To match to the standard representation of commuters, we may take p to be the number of partitions associated to the symbolization of Y, with that p then used to define the number of symbols for representation of the X dynamics. We take the distance between two symbolic sequences to be the standard metric on Σ_p, given by

$$d(\sigma, \tilde{\sigma}) = \sum_{k=0}^{\infty} \frac{\delta(\sigma_k, \tilde{\sigma}_k)}{p^k}, \tag{17}$$

where δ is the Kroneker delta.

In this setting, we may define the commuter $f : X \to Y, \quad f(x) = y$, as follows: For arbitrary x, let σ_x be the symbolic representation of x. Then let

$$\mathcal{F}(x) := \arg\min_{y \in Y} d(\sigma_x, \sigma_y), \tag{18}$$

the set of nearest points in symbol space, which are the *feasible set* for $f(x)$. Although $\mathcal{F}(x)$ is obviously non-empty, it may contain more than one element. To define the commuter, we assign

$$f(x) := \arg\min_{y \in \mathcal{F}(x)} \phi(y), \tag{19}$$

where ϕ is some appropriately chosen function that supports selection of a unique y from the feasible set. (The specifics of this selector operation are somewhat arbitrary and are related to the arbitrary choice of "zed" in the standard methodology described in [7, 8].)

We observe the following in relation to this approach for developing commuters:

- Implicit in the assignment of symbols to partition elements is that we are forcing the commuter match with respect to those regions of phase space, a fundamental source of non-uniqueness of the commuter.
- Because our interest is in comparing "nearby" dynamical systems, the idea that p symbols should be an appropriate representation for both X and Y dynamics is not unreasonable. The two likely situations are that either both dynamics use the same number of symbols *or* the one of the systems can be projected onto a smaller symbol set without "too much" loss of fidelity.
- Equation (18) enforces that the symbol sequence $\sigma_{f(x)}$ matches σ_x for as many leading symbols as possible.
- If the partition on X is not generating, then the resultant commuter must have some points where it is infinite-to-one, which associates to horizontal segments of the commuter in the 1-d setting.
- If a work (finite length symbol sequence) attainable under Y dynamics has no match in X dynamics, then an entire cylinder set in Σ_Y is not reached, which associates to the vertical gaps in the commuter for the 1-d setting.
- If the partition on Y is not generating, then (18) may be uncountably infinite even if there is an infinite length match of symbols, [11]. The resultant commuter, even when uniquely defined through (19), may be unsuitable for comparing the systems.

In application where we seek to *approximate* the commuter, this symbolic approach would require identifying preimages of partition sets. In the 1-d setting, interval arithmetic provides a suitable methodology. The higher-dimensional problem would (likely) require approximation of those preimages. Although the process cannot be continued to the limit of infinite partition refinement, a finite symbol length matching would resolve the commuter to within some required accuracy. As a counterpoint, computational complexity grows exponentially with the length of the finite symbol sequences, which may make this approach impractical for typical application problems unless only a low resolution view of the commuter is required See Fig. 5 for an illustration of this symbol matching approach in the setting of a Smale horseshoe.

B. Cycling Commuters: On Matching Using Periodic Orbits,

Matching symbol sequences between two dynamical systems, when such representations exist for each, automatically matches periodic orbits of each dynamical system. Therefore, a necessary condition for construction of a commuter is that it must "appropriately" match periodic orbits of each dynamical system. The advantage of focusing on periodic orbits is that a natural, discrete, and hierarchical method may be developed. The disadvantages are of course, the computational difficulty of constructing complete sets of periodic orbits, and the difficulty of choosing which periodic orbits to match - that is, how to define that phrase, "appropriate." Development of efficient numerical algorithms to construct hundreds, thousands, and surprisingly even hundreds of thousands, of periodic orbits has been an active area studied by many researchers, with significant advancement on modern computers, [12–15], including our own contributions, [16, 17]. Discussion of issues of complete detection [18], connections between growth rate of periodic orbits, entropy, and also construction of generating partition for symbolic dynamics directly from a presentation of complete hierarchical listings of periodic orbits can be found in [19], with related material in [20], and related techniques in, [21, 22]. There are many connections between periodic orbit structure and chaotic motion, too numerous to list completely here, but we suggest these applied works, [23, 24].

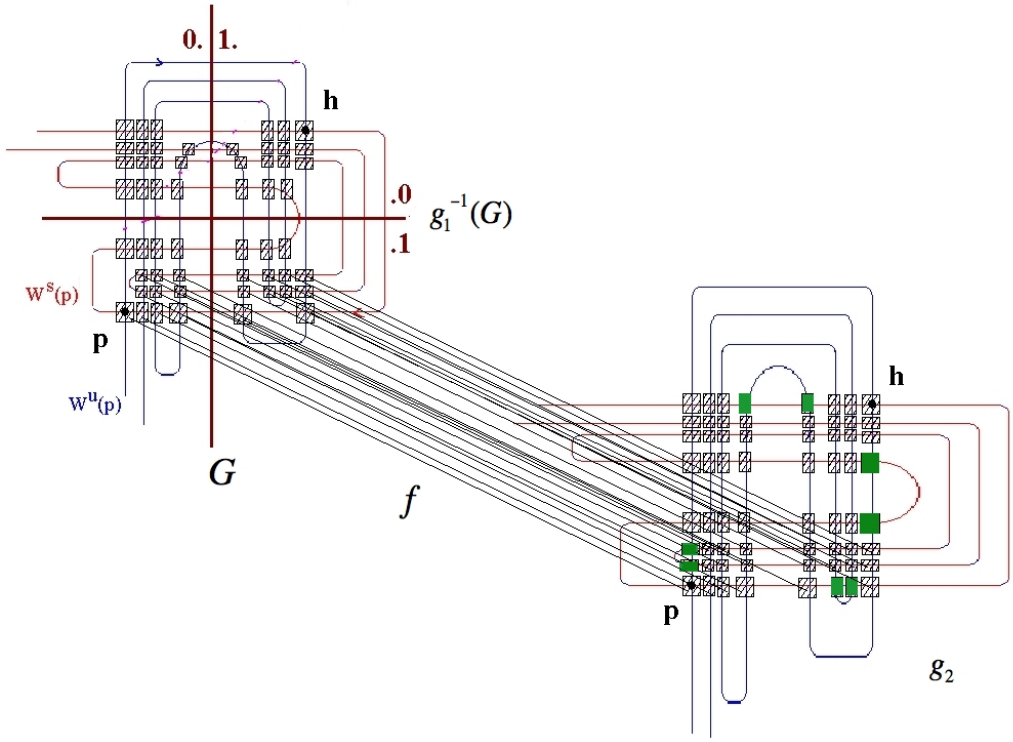

FIG. 5: Matching neighborhoods in the setting of a Smale horseshoe near a transverse intersection of a stable $W^s(p)$ and unstable $W^u(p)$ manifold of a periodic point point p. The right horseshoe includes a full shift and is fully developed, whereas, the homoclinic tangle is pre-tangency, and as such, some periodic orbits are missing. Specifically, the green solid neighborhoods in the horseshoe on the right cannot be assigned by an appropriate commuter to any neighborhoods on the left due to missing dynamics. Compare this figure to the one-dimensional setting of an assignment mapping due to missing dynamics in Fig. 3. Only a few lines are shown of the assignment mapping f for artistic reasons in order not to obscure the individual dynamics.

Matching periodic orbits in order to estimate commuters may be described as follows. Denote $x_{i,k}^m$ to be a point on the kth period-m orbit of g_1, $i = 0, 1, ...m-1$, and m is the smallest integer such that $g_1(x_{i,k})^m = x_{i,k}$. Then $\{\{x_{i,k}^m\}_{i,k}\}_{m=1}^M$ is a hierarchical finite list of periodic orbits, through period-M. Similarly, $\{y_{j,l}^m\}$ identifies a period-m orbit of g_2, and a corresponding hierarchical list, $\{\{y_{j,l}^m\}_{j,l}\}_{m=1}^M$. With this notation, a commuter f implies a matching between periodic orbits of like period. A valid commuter, restricted to the periodic orbits may be defined by matching any pair of periodic points

$$\tilde{f}(x_{i,k}^m) = y_{j,l}^m, \tag{20}$$

where $0 \leq i, j \leq m-1$ and k, l which correspond to periodic orbits are taken arbitarily but treated as fixed. To preserve the dynamic order of the periodic orbits, we additionally require that

$$g_1^q(\tilde{f}(x_{i,k}^m)) = g_2^q(y_{j,l}^m), \qquad 0 \leq q \leq m-1. \tag{21}$$

We emphasize that any circulant order of periodic orbits may be matched, and this is a source of nonuniqueness of commuters, but we prefer the order relevant to the metric topology; that is, we attempt to match points that are nearby in the obvious manner, without including notation here which denotes the matching according to the metric. This approach appears particularly relevant when we are comparing two systems that are not vastly different. Without any claims of optimality, we may use this metric topology as a guide to matching periodic orbits using a coloring scheme, similar to the one we introduced in [19], which uses the low period orbits as the backbone structure to establish a "closeness" criteria for the higher period orbits. This approach allows identification of a matching that (in aggregate) tends to minimize the distance between matched orbits, and hence, best respects the metric topology on the space. While this approach only

produces a commuter restricted to periodic orbits, it is noteworthy that periodic orbits are dense in chaotic attractors. We note that the two dynamical systems may not even have the same numbers of periodic orbits, of each order, and this is simply reflects the consequence of the impossibility of producing a one-one and onto commuter between two non-conjugate dynamical systems.

C. Computing Defect Using Symbolization

In [7, 8], we introduced the philosophy that measuring differences between two dynamical systems, $g_1 : X \to X$, and $g_2 : Y \to Y$, should be made by measuring the commuter between them. That is, rather than measuring directly the differences between two dynamical systems in terms of some norm, we endow both topological spaces X and Y with measure structure, $(\mu_1, X, \mathcal{A})$, and $(\mu_2, Y, \mathcal{B})$, and using relative measures from μ_1 and μ_2, we may directly measure a defect which defines a departure of the commuter $f : X \to Y$ from being a homeomorphism. That is, "how much" is it not one-one, onto, continuous, and/or its inverse continuous? However, the difficulty in implementing the specific defect measures, as we call the departure of f from each of the properties of homeomorphism, is that they often involve an infimum over all measurable sets with a given property, making them computationally difficult to manage. However, if there is a good symbolization of the dynamical systems, as we have discussed here, then that symbolization can be used to greatly simplify the computation of defect measure of the corresponding commuter f. Of course, the difficulty is only transfered, in that there are great technical issues in producing a generating partition for the symbolic dynamics for each dynamical system, [25–29], and *Markov Partitions* in [30]. Nonetheless, that problem of finding good symbolic partitions, whether they be Markov or simply generating, is a well studied if not fully mastered issue which is familiar to many in the field of dynamical systems [31]. A major advantage of the symbol dynamic approach is that it is, in principle, adaptable to multivariate transformations, although the narrative here is in terms of one-dimensional transformations for simplicity artistic presentation. We introduce (by example) concepts of computing defect measure through symbolization, to be discussed in greater detail elsewhere [32]. To execute this computation with symbolization, we must consider the result in a sequence of representations of the grammars of each of the dynamical systems g_1, and g_2 in terms of n-bit symbolizations on D_1 and D_2 respectively. For fixed n, the computation provides a finite precision representation of the defect. Implication of the limiting case, $n \to \infty$ is briefly discused in Appendix 7 and elsewhere.

Consider the onto defect [8], but in terms of symbolization. Let,

$$\lambda_o(f) = 1 - \frac{\overline{\mu_2}(f(D_1))}{\mu_2 D_2)}, \tag{22}$$

where now we interpret D_1 as the symbolized invariant set of g_1, in X, and D_2 is the symbolized invariant set of g_2 in Y. For measures, we assume a maximal entropy measure which simply counts symbol occurrences, with equal weight assigned for equal run lengths. The overbar represents the relative measure, of μ_2 restricted to D_2.

For example, we take the symbolization resulting from two tent maps: $g_1 = a(1 - 2|x - 1/2|)$, with $a = 1$ such that a full shift map, $s : \Sigma_2 \to \Sigma_2$ results, and $g_2 = a(1 - 2|x - 1/2|)$, such that the grammar is a subshift Σ_2' where no two zero's in a row occur[39] In Fig. 6, (compare to Fig. 3), we illustrate the adjacency matrix of each of these shifts, which being right resolvent shifts of finite type, they are exactly represented by finite graphs that happen to be deBroijn. In the picture shown, D_2 corresponds to a connected interval (in the continuum space Y), but it appears to be not connected as shown in the symbol space generated by $\sigma : [0, 1] \to \Sigma_2'$, because we have illustrated the missing words, 0.100 and 1.100 where they would appear in the Gray code ordering. So now, we simply count the onto measure, with a counting measure μ_2[40] and according to Eq. (22): In four-bit resolution, we have

$$D_1 = \{0.000, 0.001, 0.011, 0.010, 0.110, 0.111, 0.101, 0.100, 1.100, 1.101, 1.111, 1.110, 1.010, 1.011, 1.1001, 1.000\},$$

which is all possible 4-bit words in the fullshift Σ_2. Then

$$f(D_1) = \{0.000, 0.001, 0.011, 0.010, 0.110, 0.111, 0.101, 1.101, 1.111, 1.110, 1.010, 1.011, 1.1001, 1.000\},$$

where ($\{0.100, 1.100\}$ are "removed" from the list). To apply relative measure, we compute

$$f(D_1) \cap D_2 = D_2 = \{0.110, 0.111, 0.101, 1.101, 1.111, 1.110, 1.010, 1.011\},$$

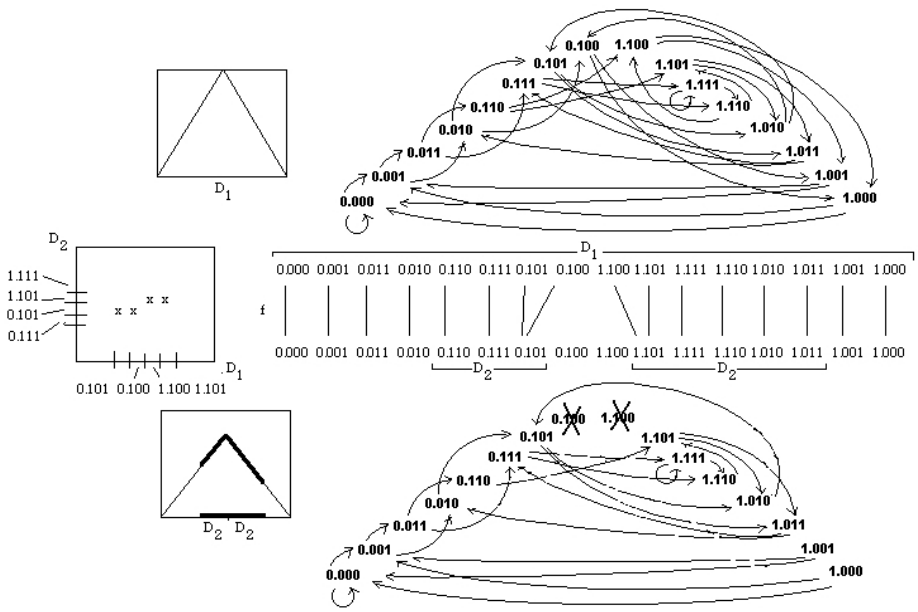

FIG. 6: This figure is the graph counter part to the assignment mapping shown in Fig. 3. **(Top) Full Shift.** Arranged left to right by the Gray code order [33] as is monotone to the symbolization of the tent map, and the graph is likewise shown to suggest the originating tent map, which is shown in the box inset on the left. All words of the deBroijn graph are allowed and generate the shift, Σ_2. **(Bottom) Golden Shift.** The Golden Mean subshift Σ_2', due to a grammar in which no two zero's occur sequentially, generated by the right resolving graph shown here and corresponding to a submaximal tent map; forbidden words are x'ed. The generating tent map is shown at the left, the notable feature being that it is submaximal ($g_2(1/2) < 1$). The invariant set, chosen as the domain D_2, is shown as the bolded lines. **(Middle) A Symbolic Assignment Plot.** The full shift (top) is assigned to the subshift (bottom). $f : X \to Y$. (**Far Left**) A symbolic representation of $f : D_1 \to D_2$. Note that in the Gray-code order topology of D_2, with $\{0.100, 1.100\}$ removed, that 0.101 and 1.101 are adjacent in D_2 reflecting that D_2 is the continuum shown in the tent, lower left, and the portion of the assignment mapping of the subdomain $f : \{0.101, 0.100, 1.100, 1.101\} \subset D_1 \to \{0.111, 0.101, 1.101, 1.111\} \subset D_2$.

because all of D_2 is the image of $f(D_1)$, which we see in the symbolic assignment mapping in Fig. 6. Hence

$$\lambda_o(f) = 1 - \frac{\overline{\mu_2}(f(D_1))}{\mu_2(D_2)} = 1 - 8/8 = 0, \tag{23}$$

because 8 out of 8 symbols are "hit."

Continuing with the example illustrated in Fig. 6, we consider the 4-bit approximation of a symbolized interpretation 1-1 defect, starting from the definition in [8]. We define $\mathcal{G}$ to be the collection of all subsets $G \subset D_1$ which satisfy 1) G is μ_1 measurable; 2) $f[G]$ is $\overline{\mu_2}$ measurable; 3) f restricted to G is $1-1$. For any such G, its complement in D_1 is $\bar{G} \equiv D_1 - G$. Then we defined the $1-1$ *defect* by

$$\lambda_{1-1}(f) := \inf_{G \subset \mathcal{G}} \left[\frac{\mu_1(\bar{G})}{2\mu_1(D_1)} + \frac{\overline{\mu_2}(f[\bar{G}])}{2\mu_2(D_2)} \right]. \tag{24}$$

In terms of symbolization, and the counting measure, the example shown in Fig. 6, $\lambda_{1-1}(f)$ becomes,

$$\lambda_{1-1}(f) = \frac{1}{2}[\frac{2}{16}] + \frac{1}{2}[\frac{2}{8}] = 3/8, \tag{25}$$

since a 4-bit representation of an optimal one-to-one set excludes $\{0.100, 1.100\}$ from D_1. Thus, $\mu_1(\bar{G}) = \mu_1(\{0.100, 1.100\}) = 2$, and $\mu_1(D_1) = 16$. Similarly, $f(\bar{G}) = \{0.101, 1.101\}$ and so $\overline{\mu_2}(f[\bar{G}]) = 2$, and again, $\mu_2(D_2) = 8$. Thus, $\lambda_{1-1}(f) \approx 3/8$ represents the 4-bit approximation. Comparing Fig. 3 to Fig. 6, we note one source of approximation error is that while in 4-bits we compute $\overline{\mu_2}(f[\bar{G}]) = 2$ since $f[\bar{G}]$ covers

$\{0.101, 1.101\}$, the the Cantor set structure indicated that $\bar{G}$ must grow as we increase resolution, as finer scale "flat spots" must be counted.

The definition of continuity requires reference to the underlying topologies of D_1 and D_2, by definition[41], and this cannot be any different for a relevant symbolized continuity defect. Here, for specificity, we specialize to to the one-dimensional dynamics of the underlying tent map transformations. The Gray code order which follows from the kneading theory, [6], illustrated in Fig. 3 generates an order topology [10] in both D_1, D_2. In [8], we concluded that the continuity defect measure may be associated with the atomic parts of the commuter, f,

$$\lambda_C(f) := \sup_{x_0 \in D_1} a(x_0), \tag{26}$$

where

$$a_\delta(x_0) := \inf_{I \supset f[\mathcal{B}(\delta, x_0)]} \frac{\mu_2\left(I \cap D_2\right)}{\mu_2(D_2)}, \text{ and, } a(x_0) := \lim_{\delta \to 0^+} a_\delta(x_0), \tag{27}$$

Interpreting on the symbol space, we note that $\mathcal{B}(\delta, x_0)$ and intervals I associate to cylinder sets with respect to the chosen topology. To construct the $n-$bit approximation of this defect, we observe that for any x_0 inside one of the symbol bins, a $\delta-$ball may be chosen to fit inside that bin. Since each bin is *always* mapped to exactly one bin by f, a single point in σ_y, an $n-$bit counting measurement of I would always measure as 1. Consequently, the sup operation of (26) must be achieved at some x_0 that lies on the boundary between two adjacent 4-symbol bins. A $\delta-$ball around such a boundary point, therefore, will intersect both of the adjacent bins. As example, if we take $x_0 = 0.5$ to be the boundary point between 0.100 and 1.100, then the smallest ball that we can consider (at 4-bit resolution) would be

$$\mathcal{B}(\delta, x_0 = (0.100, 1.100)\,.$$

Again, restricting to 4-bit resolution, the smallest I that we may choose is

$$I = f\left[\mathcal{B}(\delta, x_0)\right] = (0.101, 1.101)\,.$$

The notation on the right indicates an interval. If we *list* all the 4-bit sequences contained in that interval (with respect to the Gray code order on D_2) we find that $I_{(4)} = \{0.101, 1.101\}$, where the sequences 0.100 and 1.100 are not listed because they are not included in the topology of D_2.

In restricting ourselves to an $n-$bit representation, our $\delta-$balls and intervals are always an overestimate of the atomic part of the commuter. Observe that even when f is the identity map, we would have that counting measure $\mu_2(I \cap D_2) = 2$, because the interval endpoints would always be counted. To remove this bias, we compute are $n-$bit approximation as

$$a_{n,\delta}(x_0) := \inf_{I \supset f[\mathcal{B}(\delta, x_0)]} \frac{\mu_2\left((I - \partial I) \cap D_2\right)}{\mu_2(D_2)}, \tag{28}$$

where ∂I denotes the extreme points of the cylinder set with respect to the order topology. Applying to our example at $x_0 = 0.5$, we have that $I - \partial I = \emptyset$, yielding that $a(x_0 = 0.5) = 0$. One may verify that (for this example), the computation is the same at all other interval boundary points, so that by (26), we have that $\lambda_C(f) = 0$.

The continuity defect of the preimage, $\lambda_{C^{-1}}(f)$, is measured in the same manner [8], applied to the preimage relationship f^{-1} (noting that the inverse may not generally exist). Continuing with the 4-bit estimation example shown in Fig. 6, we focus on $y_0 = 0.5$ (because we observe that it creates the largest "gap" in the inverse mapping). Taking an $\epsilon-$ball around y_0, we create cylinder set

$$\mathcal{B}(\epsilon, y_0) = (0.101, 1.101)\,,$$

as minimal in the order toplogy on D_2 at 4-bit resolution. Computing the inverse image and finding a bounding interval in D_1 results in cylinder set $I = (0.101, 1.101)$. Then $I - \partial I = \{0.100, 1.100\}$, and we compute

$$\lambda_{C^{-1}}(f) = \frac{\mu_1\left((I - \partial I) \cap D_1)\right)}{\mu_1(D_1)} = \frac{2}{16} = 1/8.$$

In our upcoming work, [32], we will clarify in greater detail several issues only mentioned here, with particular focus on implication and treatment of the limiting case of $n \to \infty$ in a sequence of n-bit representations of symbolically encoded dynamical systems. While onto and 1-1 defects generalize simply to multivariate dynamical systems in the symbolic representation, continuity defect requires extra topological information. Continuity obviously relies much more fundamentally on the underlying phase space structure. For higher dimensional systems, the kneading theory and associated order for the one dimensional problem must be extended. We require a generalized kneading theory, for which we will discuss the role of pruning-front theory [25, 34] and the associated partial order, and the resulting order topology required to develop a symbolic continuity defect measure.

6. CONCLUSIONS

The connections drawn in this paper between commuters of maps on R^n and their associated symbolic dynamic representation reflect an important step forward in the theory of commuters and defect measure. The formulation of commuter directly on symbol space allows that we may take advantage of the vast power of the tools of symbolic representation. These theoretical advances point to several possible avenues for computer implementations suitable for finding commuters and measuring defects. These approaches need to be more completely developed and tested against a variety of problems to evaluate the utility. Our expectation is that these techniques will provide viable methods for applying commuter theory to higher dimensional problems. It should be noted that the difficulty in computing commuters and defects is alleviated in so far as the difficulty is associated to a widely understood difficulty in constructing generating partitions for general dynamical systems. In particular, our developing work [32] is directed toward a complete theory of defect measure in symbol space, advancing what we mentioned here, which has two major features to expand upon: 1) the symbolic defect measure is a finite resolution approximations based on n-bit symbolic grammar representation of the dynamical systems, 2) measurement of continuity defect measures must follow a topology on the symbol space, which in higher dimensional transformations, can be pursued in terms of the order topology based on the pruning front theory [25, 34] generalization of kneading theory [6].

7. ACKNOWLEDGMENTS

This research was supported under NSF grant DMS-0404778.

Appendix A: Example: symbolic onto-defect in the limit $n \to \infty$

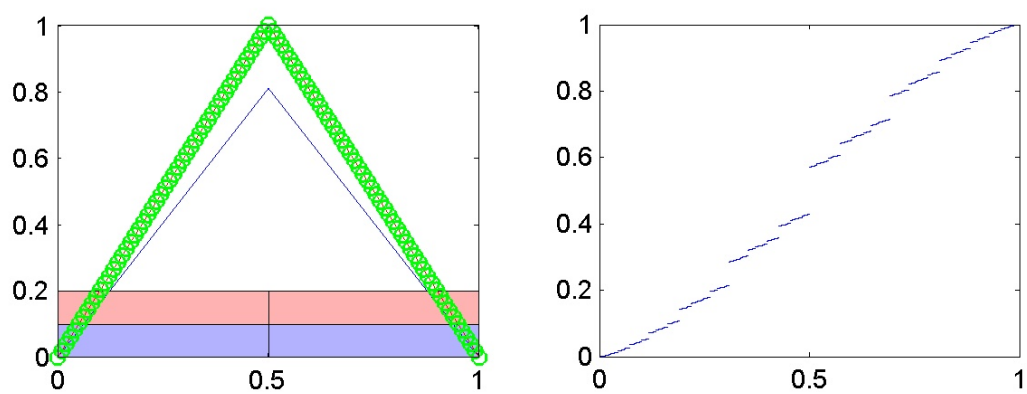

FIG. 7: Comparison of two tent maps using a commuter. Observe the self-similar structure of the commuter, with the upper and lower branches being a scaled, truncated version of the full graph.

As discussed in Sec. 5 C, symbolic defect is computable with a $n-$bit approximation to the dynamical system, with an expectation of increased precision with increasing n. In this appendix, we examine a particular example where we may compute a defect in the limit as $n \to \infty$.

Consider the measurement of the commuter formed by taking g_1 to be a symmetric tent map of height $1/2 < \nu < 1$, and g_2 to be the standard full shift symmetric tent. The commuter (illustrated in Fig. 7) is not onto, and we desire to measure that defect using the standard symbolic dynamics of these maps, where g_1 associates to subshift Σ_2' while g_2 associates to the full shift Σ_2. In particular (applying (22)), we want to evaluate

$$\lambda_o(f) = 1 - \lim_{n\to\infty} \frac{|(f(D_{1,n}))|}{|D_{2,n}|)}, \tag{A1}$$

where $|\cdot|$ is meant to indicate a counting measure and $D_{i,n}$ indicates the set of $n-$bit sequences that can be produced by the associated symbol dynamics. Because system 2 is the full shift, every sequence generated under g_1 can be correctly matched to a sequence under g_2, application of the commuter f does not change the counting, so that $|(f(D_{1,n}))| = |D_{1,n}|$.

From standard analysis of constant slope maps [4], we know that the topological entropy of system 1 is $h_{T_1} = \log(2\nu)$, while the entropy of system 2 is $h_{T_2} = \log(2)$, with entropy defined by

$$h_T = \lim_{n\to\infty} \frac{\log |D_{i,n}|}{n}. \tag{A2}$$

Using (A2) to express the counting of (A1) in terms of entropy, we have

$$\lambda_o(f) = 1 - \lim_{n\to\infty} \frac{|(f(D_{1,n}))|}{|D_{2,n}|} = 1 - \lim_{n\to\infty} \frac{e^{nh_{T_1}}}{e^{nh_{T_2}}} = 1 - \lim_{n\to\infty} \frac{(2\nu)^n}{2^n} = 1 - 0 = 1, \tag{A3}$$

for $\nu < 1$.

The implication is that in the symbolic space, the onto defect for these two maps is full measure when viewed at infinite bit death. This result is completely consistent with the computation of defect on the continuum if we assume that we measure the sets using Lebesgue measure. To briefly sketch this connection, we note that $g_1(x) = \nu\,(1 - 2|x - 1/2|)$ and $g_2(x) = 1 - 2|x - 1/2|$. Requiring that f satisfy the commutative diagram implies that it must satisfy the functional equation

$$f(x) = \begin{cases} \frac{1}{2} f(2\nu x) & 0 \le x \le 1/2 \\ 1 - \frac{1}{2} f\left(2\nu\,(1-x)\right) & 1/2 < x \le 1, \end{cases} \tag{A4}$$

which follows directly from detailed description in [8]. Let R denote the range of f. Let $S_1 = \{y | 2y \in R\}$ and $S_2 = \{y | 1 - y \in S_1\}$. Because sets S_1 and S_2 are simply scaled (by factor of 2) versions of R, we have

$$m(S_1) = m(S_2) = \frac{1}{2} m(R),$$

where $m(\cdot)$ denotes Lebesgue measure. Because of the self-similarity implied by (A4), we note that for $0 \le x \le 1/2$, f is a scaled version of itself, scaled vertically by $1/2$ and horizontally by $1/2\nu$. However, when $\nu < 1$, we horizontal scaling is not sufficient to scale the whole domain $[0, 1]$ into the interval $[0, 1/2]$, so part of that scaled copy of f is "cut off." It includes only the scaled image of $f([0, \nu])$. By symmetry, a similar argument holds for $1/2 < x \le 1$. We now bound $m(R)$ by arguing

$$m(R) = m\left(f([0, 1/2])\right) + m\left(f((1/2, 1])\right) \le \gamma\left(m(S_1) + m(S_2)\right), \tag{A5}$$

where $\gamma < 1$ accounts for the fact that a portion of the scaled set is removed. Then

$$m(R) \le \gamma m(R) \quad \Longrightarrow \; m(R) = 0 \quad \Longrightarrow \; \lambda_o(f) = 1 - 0 = 1.$$

[1] H. Poincare and R. Magini, Il Nuovo Cimento (1895-1900) **10**, 128 (1899).

[2] C. Robinson, *Dynamical systems: stability, symbolic dynamics, and chaos* (CRC press, 1999).
[3] B. Kitchens, *Symbolic dynamics: one-sided, two-sided, and countable state Markov shifts* (Springer, 1998).
[4] E. Ott, *Chaos in dynamical systems* (Cambridge university press, 2002).
[5] J. Guckenheimer and P. Holmes, *Nonlinear oscillations, dynamical systems, and bifurcations of vector fields* (Springer, 1983).
[6] R. Devaney, *An introduction to chaotic dynamical systems* (Westview Press, 2003).
[7] J. Skufca and E. Bollt, Physical Review E **76**, 26220 (2007).
[8] J. Skufca and E. Bollt, Chaos: An Interdisciplinary Journal of Nonlinear Science **18**, 013118 (2008).
[9] B. M. Douglas Lind, *An Introduction to Symbolic Dynamics and Coding* (Cambridge University Press, 1995).
[10] J. Munkres, *Topology: a first course* (Prentice-Hall Englewood Cliffs, NJ, 1975).
[11] E. Bollt, T. Stanford, Y. Lai, and K. Życzkowski, Physica D: Nonlinear Phenomena **154**, 259 (2001).
[12] O. Biham and W. Wenzel, Physical Review Letters **63**, 819 (1989).
[13] W. Wenzel, O. Biham, and C. Jayaprakash, Physical Review A **43**, 6550 (1991).
[14] F. K. Diakonos, P. Schmelcher, and O. Biham, Phys. Rev. Lett. **81**, 4349 (1998).
[15] R. L. Davidchack and Y.-C. Lai, Phys. Rev. E **60**, 6172 (1999).
[16] A. Klebanoff and E. Bollt, Chaos, Solitons and Fractals **12**, 1305 (2001).
[17] R. Davidchack, Y. Lai, A. Klebanoff, and E. Bollt, Physics Letters A **287**, 99 (2001).
[18] J. Crofts and R. Davidchack, Arxiv preprint nlin.CD/0502013 (2005).
[19] R. Davidchack, Y. Lai, E. Bollt, and M. Dhamala, Physical Review E **61**, 1353 (2000).
[20] O. Biham and W. Wenzel, Physical Review A **42**, 4639 (1990).
[21] M. B. Kennel and M. Buhl, Phys. Rev. Lett. **91**, 084102 (2003).
[22] Y. Hirata, K. Judd, and D. Kilminster, Physical Review E **70**, 16215 (2004).
[23] D. Auerbach, P. Cvitanović, J. Eckmann, G. Gunaratne, and I. Procaccia, Physical Review Letters **58**, 2387 (1987).
[24] P. Cvitanović, R. Artuso, R. Mainieri, G. Tanner, and G. Vattay, *Chaos: Classical and Quantum* (Niels Bohr Institute, Copenhagen, 2005), ChaosBook.org.
[25] P. Cvitanović, G. Gunaratne, and I. Procaccia, Physical Review A **38**, 1503 (1988).
[26] B. Hao, *Elementary symbolic dynamics and chaos in dissipative systems* (World Scientific Pub Co Inc, 1989).
[27] P. Grassberger, H. Kantz, and U. Moenig, J. Phys. A: Math. Gen **22**, 5217 (1989).
[28] M. Lefranc, P. Glorieux, F. Papo, F. Molesti, and E. Arimondo, J. Nonlinear Sci Phys Rev Lett **73**, 1364 (1991).
[29] R. Davidchack, Y. Lai, E. Bollt, and M. Dhamala, Physical Review E **61**, 1353 (2000).
[30] A. Scott, P. Christiansen, and M. Sorensen, *Nonlinear science* (Oxford University Press New York, 1999).
[31] D. J. Rudolph, *Fundamentals of Measurable Dynamics, Ergodic theory on Lebesgue spaces* (Clarendon Press, Oxford, 1990).
[32] J. S. Bollt, EM (2009).
[33] W. Press, *Numerical recipes: the art of scientific computing* (Cambridge university press, 2007).
[34] Y. Lai, E. Bollt, and C. Grebogi, Physics Letters A **255**, 75 (1999).
[35] K. Życzkowski and E. Bollt, Physica D: Nonlinear Phenomena **132**, 392 (1999).
[36] We call any f which satisfies the Eq. (2) a *commuter, regardless of whether it is a homeomorphism or not.*
[37] If $g_1(x) = 4x(1-x)$ and $g_2(x) = if(x < 1/2, 2x, 2(1-x))$, by $f(x) = (1 - cos(\pi x))/2$, which is not just a homeomorphism, but is actually a stronger form of equivalence, as it is a diffeomorphism, which carries smoothness properties between the systems including Lyapunov exponents.
[38] A subshift Σ'_p is a topologically closed and shift map invariant subset of the full shift $\Sigma_p = \{\sigma|\sigma = ...\sigma_{-2}\sigma_{-1}.\sigma_0\sigma_1\sigma_2...\}$, the set of all (bi)infinite symbolic sequences from a given alphabet, $\{0, 1, 2, ..., p-1\}$, [3].
[39] No two zero's in a row this is the so-called "golden-shift", [11, 35], since the spectral radius of the corresponding adjacency matrix is the golden mean, $\gamma = \frac{1+\sqrt{5}}{2}$), and its topological entropy, $h_T = \ln\gamma$.
[40] This counting measure is actually the maximal entropy measure.
[41] A continuous functions requires that pre-images of open sets are open sets, [10].